Sains Malaysiana 55(10)(2026): 1725-1734
http://doi.org/10.17576/jsm-2026-5510-11

Synthesis of Cationic Copolymers P(DMA$^+$-*co*-HEMA) for Lectin Immobilisation

(Sintesis Kopolimer Kationik P(DMA$^+$-*co*-HEMA) untuk Imobilisasi Lektin)

MUHAMMAD ASHRAF SHAHIDAN[1], NOOR HIDAYAH CHE LAH[2] & NUR NABILAH SHAHIDAN[2,*]

[1]*Faculty of Science and Technology, Universiti Kebangsaan Malaysia, 43600 UKM Bangi, Selangor, Malaysia*
[2]*Faculty of Bioengineering and Technology, Universiti Malaysia Kelantan, Jeli Campus, Locked Bag No. 100, 17600 Jeli, Kelantan, Malaysia*

Received: 29 May 2026/Accepted: 25 September 2026

*Corresponding author; email: nabilah@umk.edu.my

ABSTRACT

The study aims to synthesise polycationic polymer, P(DMA$^+$-*co*-HEMA) with hydroxyl-functional group for lectin immobilisation. To investigate the effect of hydroxyl group spacing on protein immobilisation, four copolymers were synthesised using two [DMA]:[HEMA] molar ratios (1:1 and 3:1) and two different number-average molecular weights (M_n), namely L1$^+$:1, L3$^+$:1, H1$^+$:1 and H3$^+$:1. Successful copolymer formation and quaternisation of the amine group were confirmed by ^{1}H NMR spectroscopy, which displayed a distinct downfield shift upon amine group quaternisation. As the [DMA]:[HEMA] ratio increases, the zeta potential (ζ)) increases while the hydrodynamic diameter (D_h) decreases. Conversely, as M_n increases, ζ decreases while D_h increases. The highest D_h (353.83 nm) and ζ (62.13 mV) were observed for copolymer H1$^+$:1 and L3$^+$:1, respectively. The chemical bath deposition method was applied to produce thin polycationic films on quartz substrate, followed by immobilisation of a lectin, Concanavalin A (Con A) via electrostatic interaction. Con A immobilisation was then characterised using atomic force microscopy (AFM). Copolymer H3$^+$:1 showed the R_a of 2.838 nm following Con A immobilisation, suggesting that higher cationic group density may promote more homogeneous protein coverage. These findings indicate that the precise regulation of hydroxyl groups within polycationic scaffolds serves an effective strategy for achieving high-density protein immobilisation, with significant implications for bioassay and biosensing applications.

Keywords: ATRP; DMA; HEMA; lectin; polycationic

ABSTRAK

Penyelidikan ini dijalankan bertujuan untuk mensintesis polimer polikationik, P(DMA$^+$-*co*-HEMA yang mempunyai kumpulan berfungsi hidroksil untuk digunakan dalam pemegunan lektin. Untuk mengkaji kesan penjarakan kumpulan hidroksil terhadap pemegunan protein, empat kopolimer disintesis menggunakan dua nisbah molar [DMA]:[HEMA] (1:1 and 3:1) serta nilai berat purata (M_n) yang berbeza dan dipanggil sebagai L1$^+$:1, L3$^+$:1, H1$^+$:1 dan H3$^+$:1. Sintesis kopolimer dan kuaternisasi pada kumpulan aminanya disahkan menggunakan spektroskopi ^{1}H NMR yang menunjukkan penurunan isyarat. Nilai potensi zeta (ζ) didapati meningkat, manakala saiz diameter hidrodinamik (D_h) didapati menurun dengan peningkatan nisbah [DMA]:[HEMA]. Sebaliknya, peningkatan M_n menyebabkan penurunan nilai ζ dan peningkatan nilai D_h. Nilai D_h (345.89 nm) dan ζ (61.75 mV) tertinggi masing-masing dicatatkan oleh kopolimer H1$^+$:1 dan L3$^+$:1. Seterusnya, teknik pemendapan kubang kimia digunakan untuk menghasilkan saput nipis polikationik pada substrat kuarza, disusuli dengan pemegunan lektin Concanavalin A (Con A) melalui interkasi elektrostatik. Pemegunan Con A dicirikan menggunakan teknik mikroskopi daya atom (AFM). Kopolimer H3$^+$:1 menunjukkan nilai purata kekasaran (R_a) tertinggi selepas pemegunan Con A iaitu 2.838 nm, mencadangkan ketumpatan kumpulan kationik yang tinggi pada kopolimer dapat meningkatkan liputan protein yang lebih seragam. Keputusan daripada kajian ini mencadangkan bahawa pengawalaturan yang jitu terhadap kumpulan hidroksil pada perancah polikationik dapat digunakan sebagai strategi yang berkesan untuk pemegunan protein berketumpatan tinggi serta mempunyai implikasi yang signifikan untuk aplikasi bioasai dan biopenderia.

Kata kunci: ATRP; DMA; HEMA; lektin; polikationik

INTRODUCTION

Over the past decade, significant interest has emerged in utilizing polycation-coated surfaces to immobilize proteins such as antibodies and enzymes for diverse applications ranging from antifouling and protein purification to clinical diagnostics (Duan et al. 2026; Linssen et al. 2024;

Marcelino et al. 2023; Popova, Zvereva & Borisov 2023; Soares et al. 2026). However, maintaining the immobilised protein activity remains highly challenging as high density of cationic charges can distort native protein structures, leading to a loss of biological function and causing thick, uncontrolled aggregation instead of a uniform monolayer (Tardy et al. 2021). To overcome these limitations, research has transitioned from simple electrostatic binding toward highly tailored, custom-engineered interfaces (Atif & Balasini 2024; Wang et al. 2025).

Atomic transfer radical polymerisation (ATRP) is a polymerisation technique that offers precise control over size and functionality. It has been used for the polymerisation with variety of functional monomers such as acrylic acid and methacrylate (Lorandi et al. 2020; Szewczyk-Łagodzińska et al. 2023). ATRP operates through a reversible redox equilibrium catalysed by a transition metal complex, which dynamically switches between its lower and higher oxidation states. This controlled polymerisation mechanism uses an alkyl halide initiator to generate active radical species that propagate chain growth before rapidly deactivating them back into a dormant state (Shahidan et al. 2011). By keeping the concentration of active radicals systematically low throughout the reaction, this cycle successfully suppresses termination pathways to yield highly uniform, well-defined polymeric structures with narrow molecular weight distributions (Carmali et al. 2017). Tailored polymer brushes synthesised via ATRP have been successfully grafted onto gold or glass surfaces to facilitate the immobilization of biomolecules like protein (Degirmenci et al. 2022; Gajos et al. 2025; Hucknall et al. 2009).

Lectins are a diverse class of proteins or glycoproteins that contains carbohydrate recognition domain (CRD) that are not of immune origin. Unlike carbohydrate-specific enzymes, they specifically and reversibly bind to carbohydrate without changing or modifying the carbohydrate structure. These properties can be exploited in lectin microarray development, which when combined with florescence-based detection, enables sensitive high-throughput glycan profiling. Traditionally, lectins can be immobilised onto glass substrate surface in lectin microarray development via covalent approaches include aldehyde-functionalized surfaces and epoxy-activated glass slides. While covalent immobilization chemistries provide high chemical stability and permanent tethering of lectins onto glass substrate, they are usually costly and can cause denaturation to the lectins due to the use of harsh and reactive reagents such as glutaraldehyde and epoxy (Prabhakar et al. 2025; Yang et al. 2024). Alternatively, charge-based strategies offer a more cost-effective approach for immobilising lectins onto glass substrates, while simultaneously providing a favourable microenvironment that preserves their native structural stability, in the presence of certain functional group such as hydroxyl.

In this study, atom transfer radical polymerization (ATRP) was employed to synthesise well-defined copolymers. 2-hydroxyethyl methacrylate (HEMA) was selected as a comonomer due to its pendant hydroxyl side chains that can stabilise the immobilised protein. By systematically varying the DMA:HEMA monomer ratio and polymer molecular weight (M_n), we investigated the influence of hydroxyl group spacing on protein immobilisation, as well as the cationic charge density. Using Concanavalin A (Con A), a lectin extracted from jack bean (*Canavalia ensiformis*) that is widely utilised for glycoprotein analysis as a model protein, we demonstrated the straightforward electrostatic tethering of the cationic copolymer onto the anionic surface of quartz. Ultimately, this work presents a novel strategy for fabricating polycationic polymer, poly(N,N-dimethylaminoethyl methacrylate-stat-hydroxyethyl methacrylate) or P(DMA^+-*co*-HEMA), with precisely controlled hydroxyl densities tailored for high-density protein immobilisation.

MATERIALS AND METHODS

CHEMICALS

2-(*N,N*-Dimethylamino)ethylmethacrylate (DMA, 98%, Sigma-Aldrich) and 2-hydroxyethyl methacrylate (HEMA, ≥99%, Sigma-Aldrich) were vacuum distilled twice and stored at 4 °C. 2,2-bipyridine (bpy, 99%, Sigma-Aldrich). Copper (I) bromide (Cu(I)Br), iodomethane (CH_3I), ethyl α-bromoisobutyrate (EB*i*B), concanavalin A (Con A) were all purchased from Sigma-Aldrich and used as received. Methanol was purchased from Fisher Scientific whilst sodium phosphate ($Na_3PO_4.12H_2O$) purchased from HmbG Chemicals. Deionised water was used in all reagent preparation.

SYNTHESIS AND QUARTERNISATION OF P(DMA-*co*-HEMA)

The P(DMA^+-*co*-HEMA) was synthesised via atom transfer radical polymerization (ATRP), following the protocols described by Chen et al. (2004) and Liu et al. (2008), which involve two general steps as shown in Figure 1. Step I was the synthesis of P(DMA-*co*-HEMA) using DMA and HEMA as monomers. Step II was the quaternisation of P(DMA-*co*-HEMA) using excess CH_3I to produce P(DMA^+-*co*-HEMA).

P(DMA^+-*co*-HEMA) were synthesised at two different [DMA]:[HEMA] molar ratios (1:1 and 3:1) to modulate the cationic charge density. To vary the number-average molecular weight (M_n), the monomer concentrations for the high molecular weight series (H) were doubled compared to the low molecular weight series (L) (Table 1). Accordingly, the sample nomenclature indicates both parameters; for example, H3:1 denotes a high M_n polymer synthesized with a 3:1 [DMA]:[HEMA] feed ratio.

Step I is the synthesis of P(DMA-*co*-HEMA) via ATRP. The P(DMA-*co*-HEMA) preparation for L1:1 was as follows: A solution consisting of DMA (7.55 g), HEMA (6.25 g), bpy (0.63 g), EB*i*B (0.39 g) and 15 mL of methanol in a Schlenk flask and purged with argon for 40 min with continuous stirring at room temperature. The freeze-thaw-pump cycle was repeated three times. During the final cycle, Cu(I)Br (0.29 g) was added under argon purging to initiate the polymerisation at room temperature. After 20 h, the reaction was terminated by exposure to air. Then, the reaction mixture was diluted with 1:1 ratio of water to methanol and passed through an alumina column to remove the Cu(II) Br and bpy. After that, the solution was evaporated overnight to remove the methanol and freeze-dried. Other copolymers (L3:1, H1:1 and H3:1) were prepared accordingly to the component concentration stated in Table 1.

The quaternisation of L1:1 to L1$^+$:1 was performed as follows: The P(DMA-*co*-HEMA) (0.9 g) was added to the mixture of solution containing 6 mL deionised water and 19 mL methanol while stirring. Then, the polymer was adjusted to pH 8.8 using 0.1 M sodium hydroxide. After that, CH_3I (0.35 mL) was added, and stirred for 24 h at room temperature.

CON A IMMOBILISATION

To immobilise Con A, first the P(DMA$^+$-*co*-HEMA) thin-film was deposited onto 10 mm × 5 mm quartz substrates using chemical bath deposition (CBD) method. The cationic polymer was deposited by immersing the quartz substrates in 1 mL of 0.01 wt % P(DMA$^+$-*co*-HEMA) polymer solution and left to dry at room temperature. Then, the quartz substrate was immersed in 0.1 M sodium phosphate, pH 8.2, containing 1 µM Con A for 24 h at room temperature. After that, the quartz substrate was washed with both sodium phosphate and deionised water, three times each to remove unbound Con A, and finally was dried under the flow of argon.

TABLE 1. Components ratio and concentration for the synthesis of P(DMA^+_x-*co*-HEMA$_y$)

P(DMA^+_x-*co*-HEMA$_y$)	[DMA]: [HEMA] ratio	[DMA]/ [HEMA]/[EBiB]/ [CuBr]/ [bpy] (mM)
L1$^+$:1	1:1	24/24/1/1/2
H1$^+$:1	1:1	55/46/1/1/2
L3$^+$:1	3:1	35/12/1/1/2
H3$^+$:1	3:1	73/24/1/1/2

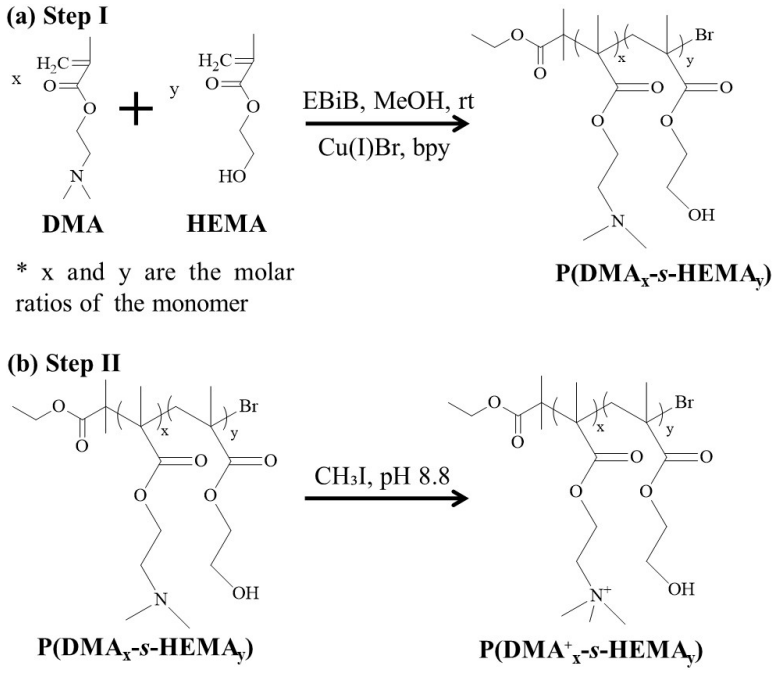


FIGURE 1. Schematic diagram for a) synthesis of P(DMA-*co*-HEMA), b) quaternisation of P(DMA-*co*-HEMA)

^{1}H NMR SPECTROSCOPY

^{1}H Nuclear Magnetic Resonance (NMR) spectra were measured using a Bruker 400 MHz spectrometer. The synthesis of P(DMA-*co*-HEMA) were analysed using deuterated chloroform ($CDCl_3$), and P(DMA$^+$-*co*-HEMA) were analysed using deuterium oxide (D_2O) as solvent. The chemical shifts were reported using TMS as internal reference.

DYNAMIC LIGHT SCATTERING AND ZETA POTENTIAL

The hydrodynamic diameter (D_h) and zetapotential (ζ) measurements were performed using a Malvern Zetasizer. The polymer concentration prepared for the measurements is 0.1 wt % in deionised water for D_h and in 1 mM NaCl for ζ measurement at 25 °C.

ATOMIC FORCE MICROSCOPY (AFM)

The surface morphology of blank quartz and thin film before and after Con A immobilisation was visualised using AFM, NX10. The images were recorded in tapping mode. The scan sizes ranged from 0 to 2 µm at a scanning rate of 0.69 Hz. The average roughness (R_a) value and was calculated using AFM analysis software (XEI, v. 4.3.4, Park Systems Corporation).

FOURIER TRANSFORM INFRARED (FT-IR) SPECTROSCOPY

A Perkin Elmer Spectrum 400 FT-IR/NIR operated in attenuated total reflectance (ATR) mode was used to detect the functional groups present on thin-film and immobilised thin-film. All FT-IR spectra were collected in the wavenumber range of 4000–400 cm^{-1} using an analysis software (OMNIC, v. 1.02, Thermo Fisher Scientific).

RESULTS AND DISCUSSION

SYNTHESIS AND CHARACTERIZATION OF P(DMA$^+$-*co*-HEMA) COPOLYMERS

The P(DMA-*co*-HEMA) was synthesised by ATRP method using Eb*i*B as initiator. The copolymer is abbreviated as H*x*:*y* or L*x*:*y*, where H and L refer to high or low M_n and *x*:*y* refers to the molar ratio of DMA to HEMA. In this study, P(DMA-*co*-HEMA) with two different molar ratios was prepared to investigate the effects of hydroxyl spacing on Con A immobilisation.

The synthesis of P(DMA-*co*-HEMA) was characterised by ^{1}H NMR using solvent $CDCl_3$ to determine the structural polymer. The signals representing the proton are shown in Figure 2 and each group of absorption peaks were marked. The NMR spectrum shows peaks at 4.0 ppm ($COOCH_2$ for both DMA and HEMA unit), 2.6 ppm (CH_2CH_2 for DMA unit), 2.3 ppm (CH_2CN_2 for DMA unit) and 3.8 ppm (CH_2CH_2OH for HEMA unit), as reported by Muranaka and Okada (2009) and Ni et al. (2017). Therefore, the synthesised copolymers L1:1, H1:1, L3:1 and H3:1 was identified. As shown in Figure 2(a), the intensity and resolution of the split methyl resonance (peak c) become more pronounced with an increasing concentration of DMA units in the polymer chain. This is consistent with the fundamental principle of ^{1}H NMR spectroscopy, where the integrated peak area is directly proportional to the molar concentration of the chemical species (Izunobi & Higginbotham 2011).

The quaternisation of amines by alkyl halides (CH_3I) is known as the Menschutkin reaction, which converts the tertiary amines group of DMA into the quaternary amine. Figure 3 shows the ^{1}H NMR spectrum of the synthesised copolymers L1$^+$:1, H1$^+$:1, L3$^+$:1 and H3$^+$:1 in D_2O solvent. The ^{1}H NMR spectrum shows the peak at 4.5 ppm corresponding to the $COOCH_2$ group in DMA and HEMA units. The peak at 4.0 ppm was attributed to CH_2CH_2OH for HEMA unit, the peak at 3.8 ppm was attributed to CH_2CH_2 for DMA unit, and the peak at 3.2 ppm was attributed for $CH_2CN_3^+$ for DMA unit. After quaternisation, a downfield shift was observed for peaks a/d, b, c, and e, resulting from the de-shielding of polymer chain protons when the amine groups were converted into quaternary ammonium ions. In Figure 3, the peak c at 3.2 ppm corresponded to the six dimethylamino protons of the DMA after quaternisation. The height and splitting of proton (methyl) peaks at peak c become slightly evident with an increased concentration of DMA units (red arrow).

The effect of the monomer ratio on the zeta potential of P(DMA$^+$-*co*-HEMA) was investigated (Figure 4). The zeta potential increased with higher DMA molar ratios, yielding values of 20.83 mV and 62.13 mV for L$^+$1:1 and L$^+$3:1, respectively. The same trend was observed for H$^+$1:1 and H$^+$3:1, with values of 14.48 mV and 28.1 mV, respectively. These positive values are directly attributed to the cationic quaternary ammonium groups on the polymer chain. Previously, Shahidan et al. (2011) reported a zeta potential of 20.0 mV for a 1:1 [DMA]:[HEMA] ratio, noting that this value approximately doubled when the DMA molar ratio was increased three times. From the zeta potential values, the [DMA]:[HEMA] ratio of 3:1 shows good stability compared to 1:1 with the copolymer L3$^+$:1 showing the highest stability followed by H3$^+$:1. A value above +30 mV indicates that the polymer chains have high positive charge density which keeps them well-dispersed via electrostatic repulsion, whilst a zeta potential value of 20 to 30 mV is considered moderately stable (Wu et al. 2026; Yang & Chang 2025). The hydrodynamic diameter D_h increases as M_n increases, where L1$^+$:1 and H1$^+$:1 show D_h increments from 170.55 nm to 353.83 nm, respectively. Whereas D_h for L3$^+$:1 and H3$^+$:1 increases from 64.30 nm to 320.00 nm. When DMA molar ratios are higher, D_h also decreases from 170.55 nm to 62.13nm for L1$^+$:1 and L3$^+$:1, respectively. This trend is also observed for H1$^+$:1 and H3$^+$:1, where the D_h decreases from 353.83 nm to

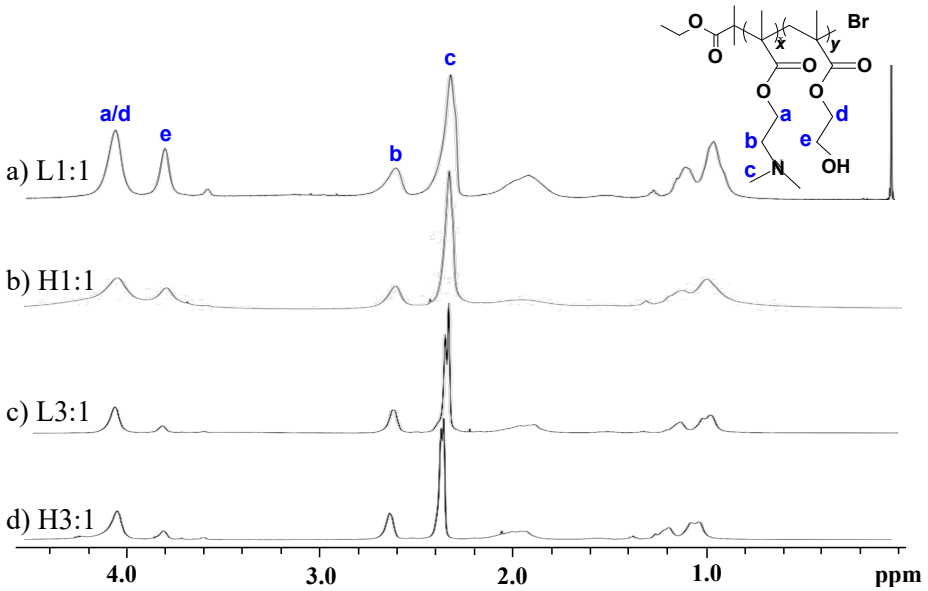


FIGURE 2. [1]H NMR spectra of the synthesised polymer a) L1:1, b) H1:1, c) L3:1 and d) H3:1

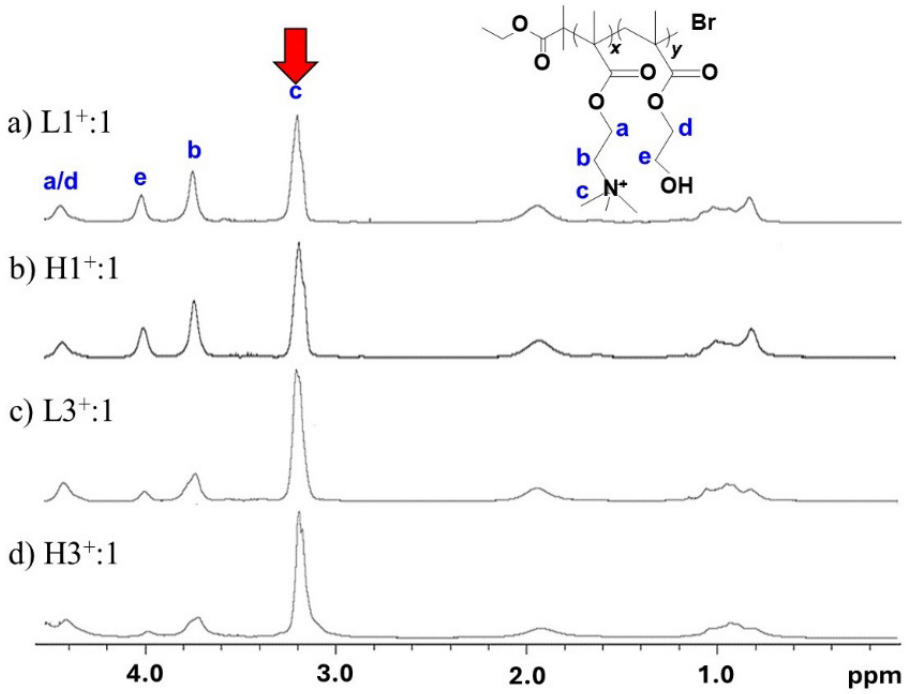


FIGURE 3. [1]H NMR spectrum of the quaternised copolymer a) L1[+]:1, b) H1[+]:1, c) L3[+]:1 and d) H3[+]:1

320.00 nm. This suggests that higher [DMA]:[HEMA] ratio promotes tighter intramolecular electrostatic condensation, decreasing the D_h (Avazverdi et al. 2023; Devarajan et al. 2022).

CON A IMMOBILISATION

The surface topographies of the synthesised P(DMA[+]-*co*-HEMA) thin films were characterised via AFM (Figure 5). The copolymer L1[+]:1 formed a highly uniform, smooth coating with an R_a value of 0.233 nm (Figure 5(a)), whereas its higher molecular weight counterpart, H1[+]:1, showed increased surface roughness with an R_a of 0.345 nm (Figure 5(c)). The topographical change intensified at higher [DMA]:[HEMA] ratios, resulting in R_a values of 0.520 nm for L3[+]:1 and 0.674 nm for H3[+]:1 (Figure 5(b) and 5(d)). These demonstrate that a higher M_n and more cationic

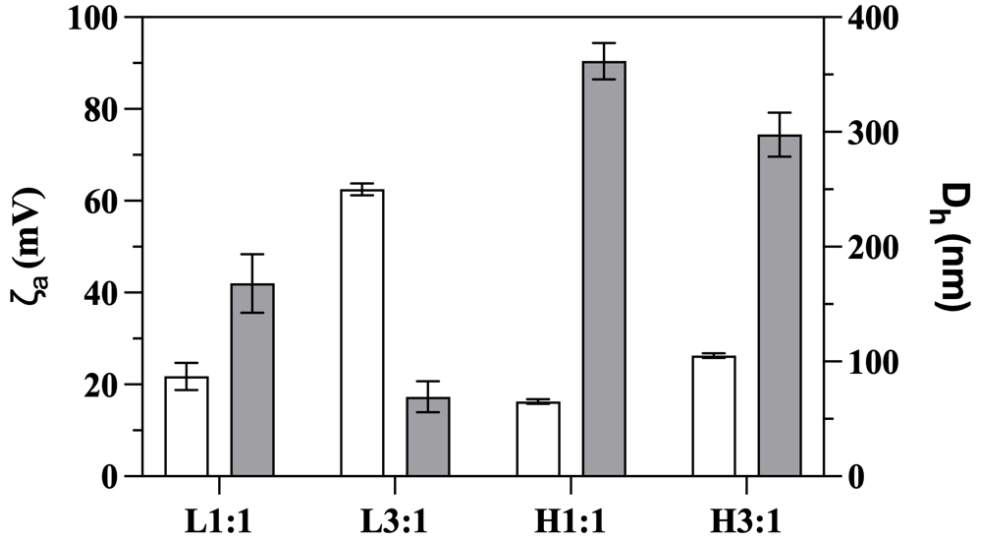


FIGURE 4. Physicochemical characterisation and structural design of P(DMA$^+$-*co*-HEMA) polymers. Apparent zeta potential (ζ_a, white bars, left axis) and hydrodynamic diameter (D_h, grey bars, right axis) across polymer variants differing in chain length (L vs. H) and cationic charge ratio (1:1 vs. 3:1). Data are presented as mean ± SD (n=3)

macromolecular chains directly increased surface roughness non-uniformity. An increased [DMA] feeding ratio yields a higher concentration of localised cationic charges, optimising electrostatic anchoring across the anionic quartz interface (Bekir et al. 2023; Shin, Roberts & Santore 2001). Figure 5(e)-5(h) shows the change in topology when Con A was immobilised on the thin film. The L1$^+$:1, H1$^+$1, L3$^+$:1, and H3$^+$:1 R_a values increase to 1.739 nm, 1.967 nm, 1.036 nm, and 2.997 nm, respectively.

Figure 5(e) and 5(f) (lower molecular weight series) and Figure 5(g) and 5(h) (higher molecular weight series) show that Con A immobilised on the thin films becomes rougher as molecular weight increases, where the R_a value for L1$^+$1 and H1$^+$:1 increases from 0.233 nm to 0.345 nm and the R_a value for L3$^+$1 and H3$^+$:1 increases from 0.520 nm to 0.674 nm. Higher molecular weight polymers may create a thicker, more flexible matrix with extended loops and tails. Therefore, when Con A is immobilised on these chains, it forms multilayered clusters and irregular domain aggregates, increasing peak-to-valley height variations. Another contribution to surface roughness is the nature of the polymer; here the copolymers are cationic. Because Con A is negatively charged, electrostatic binding drove its immobilisation. Interestingly, when Con A is immobilised on L3$^+$:1, Con A binds uniformly across the surface in a smooth monolayer, suppressing vertical aggregation and resulting in the lowest roughness. This may be due to the high charge and shorter chain length, which constrain polymer chains and force the surface brush into a flattened, electrostatically compact conformation (Farhan, Azzaroni & Huck 2005; Sakata, Inoue & Ishihara 2016). In contrast, H3$^+$:1 shows strong electrostatic binding combined with long polymer chains, causing dense, uneven protein clustering. The polymer-protein complexes protrude vertically, creating a dense array of sharp nanoscale features and the maximum roughness (2.838 nm). Some aggregation (>10 nm) was observed, due to the high pH (pH > 8) used during immobilisation. Con A exists as tetramer at pH between 5.6 - 7.4 and known to form higher aggregates at higher pH while fully retaining its binding affinity (Xu et al. 2017). In this aggregated state, Con A effectively interacts with multivalent ligands such as cell-surface glycans. This capability was demonstrated by Vetri et al. (2010), who successfully utilised aggregated Con A at pH 9 to capture cells in growth media. Concurrently, the silanol groups on the quartz surface undergo complete deprotonation at this pH (Gamba et al. 2025), creating a negatively charged substrate that strongly promotes electrostatic copolymer adsorption. Both surface topologies shown in Figure 5(e) and 5(h) are similar to the result reported by Hoang et al. (2019), where different sizes of small (less than 10 nm) and segregated lectin clusters were observed when immobilising Con A on quartz surface via silanisation, indicating the presence of different oligomeric states of Con A (monomer-tetramer). This suggested that H3$^+$:1 has a high number of functional groups that attract more Con A. The P(DMA$^+$-*co*-HEMA) with a ratio of 1:1 was affected by the D_h of P(DMA$^+$-*co*-HEMA).

The immobilised Con A on the P(DMA$^+$-*co*-HEMA) deposited thin-film observed by AFM is further confirmed by FTIR analysis. The N-H from the P(DMA$^+$-*co*-HEMA) thin-film shows a peak in the range of 3400 cm^{-1}. Figure 6(a) and 6(b) shows the Con A immobilised on H1$^+$:1 and L1$^+$:1. The magnified spectra

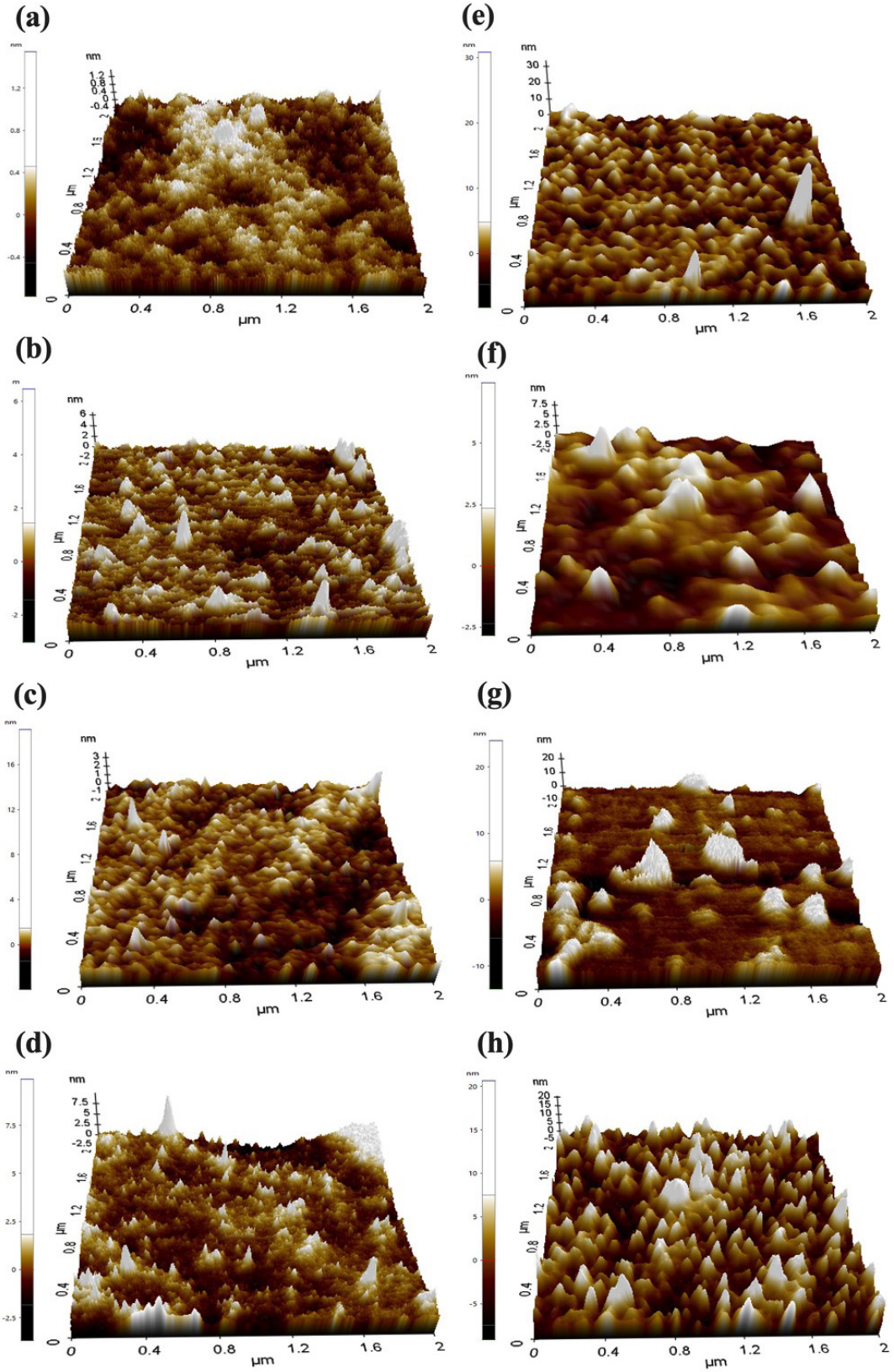


FIGURE 5. 3D Atomic Force Microscopy (AFM) topography images (2 µm × 2 µm scan size) of P(DMA$^+$-*co*-HEMA) thin films on quartz substrates before and after Concanavalin A immobilization. (a–d) Bare copolymer thin films: (a) L1$^+$:1, (b) L3$^+$:1, (c) H1$^+$:1, and (d) H3$^+$:1. (e–h) Corresponding surfaces following electrostatic immobilization of Concanavalin A (Con A): (e) L1$^+$:1 + Con A, (f) L3$^+$:1 + Con A, (g) H1$^+$:1 + Con A, and (h) H3$^+$:1 + Con A

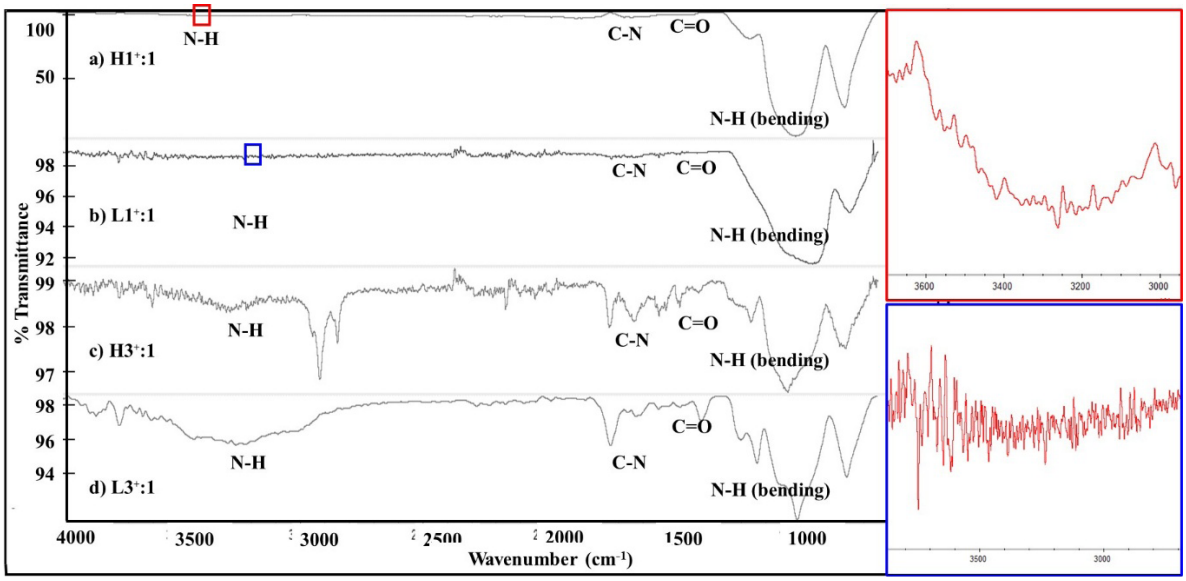


FIGURE 6. FTIR spectra of immobilised Con A on P(DMA$^+$-*co*-HEMA) thin film of a) H1$^+$:1, b) L1$^+$:1, c) H3$^+$:1, and d) L3$^+$:1

for (red and blue boxes) show a small peak between 3000 cm^{-1} and 3500 cm^{-1} corresponding to the N-H stretching band. The small peak indicated that the amount of the NH group was minuscule, possibly due to a similar number of Con A and N-H from the polymer (Mayerhöfer 2004). The N-H band are more distinct as the [DMA]:[HEMA] ratio increases from 1:1 to 3:1, as shown in Figure 6(c) and 6(d).

CONCLUSIONS

In this study, we successfully synthesised well-defined P(DMA$^+$-*co*-HEMA) copolymers using two different DMA:HEMA molar ratios using ATRP method. The NMR spectra showed P(DMA-*co*-HEMA) peak of 4.0, 3.8, 2.6, and 2.3 ppt of $COOCH_2$ (DMA, HEMA unit), CH_2CH_2OH (HEMA unit), CH_2CH_2, and $CNCH_3$ (DMA unit), respectively, which confirmed the expected copolymer compositions. Successful quaternization of the amine segments was further verified by a clear downfield shift in these signals, a direct consequence of proton de-shielding. We also found that increasing the DMA molar fraction resulted in a concomitant rise in NMR proton signal intensities, positive zeta potentials and thin-film surface roughness, confirming the targeted enrichment of cationic segments. These elevated zeta potentials indicate that the P(DMA$^+$-*co*-HEMA) thin films can anchor robustly to negatively charged biomolecules via strong electrostatic interactions. Notably, H3$^+$:1 thin film displayed the most pronounced increase in surface roughness following Con A immobilisation, but quantitative determination of the surface-bound protein density using standard colorimetric assays such as Bradford or BCA assay remains necessary to confirm total protein loading to the thin-film surface. This trend strongly suggests that the 3:1 composition yields an expanded active surface area, a higher density of operational binding sites, and an optimized spacer length compared to variations with lower DMA content. This study shows that precisely modulating the concentration of the hydroxyl groups within the polycationic scaffolds offers an effective strategy for high-density protein immobilization, which is useful for bioassay and biosensor applications.

ACKNOWLEDGEMENTS

We would like to thank the Ministry of Higher Education (MOHE), Malaysia, for providing financial support to this project (FRGS/A08.00/00319A/002/2015/00028), Universiti Malaysia Kelantan (UMK) and Centre of Research and Instrumentation Management (CRIM), Universiti Kebangsaan Malaysia (UKM) for the facilities on the instrumentation and analysis.

REFERENCES

Atif, M. & Balasini, A. 2024. Mixed polymer brushes for controlled protein adsorption: State of the art and future prospective. *Materials Advances* 5(4): 1420-1439.

Avazverdi, E., Mirzadeh, H., Ehsani, M. & Bagheri-Khoulenjani, S. 2023. Polysaccharide-based polyampholyte complex formation: Investigating the role of intra-chain interactions. *Carbohydrate Polymers* 313: 120836.

Bekir, M., Brückner, C., Zauscher, S. & Gradzielski, M. 2023. Polyelectrolyte brushes affect the adsorption kinetics of nanoparticles onto lipid membranes. *Colloids and Surfaces A: Physicochemical and Engineering Aspects* 677: 132354.

Carmali, S., Murata, H., Amemiya, E., Matyjaszewski, K. & Russell, A.J. 2017. Tertiary structure-based prediction of how ATRP initiators react with proteins. *ACS Biomaterials Science & Engineering* 3(9): 2086-2097.

Chen, X.Y., Armes, S.P., Greaves, S.J. & Watts, J.F. 2004. Synthesis of hydrophilic polymer-grafted ultrafine inorganic oxide particles in protic media at ambient temperature via atom transfer radical polymerization: Use of an electrostatically adsorbed polyelectrolytic macroinitiator. *Langmuir* 20(3): 587-595.

Degirmenci, A., Yilmaz-Becer, G., Sanyal, R. & Sanyal, A. 2022. 'Clickable' polymer brush interfaces: Tailoring monovalent to multivalent ligand display for protein immobilization and sensing. *Bioconjugate Chemistry* 33(9): 1672-1684.

Devarajan, D.S., Rekhi, S., Nikoubashman, A., Kim, Y.C., Howard, M.P. & Mittal, J. 2022. Effect of charge distribution on the dynamics of polyampholytic disordered proteins. *Macromolecules* 55(20): 8987-8997.

Duan, H., Chen, J., Frank, F., Shen, W. & Chen, Y. 2026. Nanoscale protonation limits and charge density in polymer films govern the activity of immobilized LacZ under acid stress. *Nanoscale* 18(26): 13769-13780.

Farhan, T., Azzaroni, O. & Huck, W.T.S. 2005. AFM study of cationically charged polymer brushes: Switching between soft and hard matter. *Soft Matter* 1(1): 66.

Gajos, K., Lishchynskyi, O., Dąbczyński, P., Tymetska, S., Bodek, Ł., Shymborska, Y., Janiszewska, N., Stetsyshyn, Y. & Budkowski, A. 2025. Integrating protein resistance and bioconjugation in P(OEGMA-*co*-MAA) brushes for biosensing and cell culture: ToF-SIMS profiling and antibody characterization. *ACS Applied Materials & Interfaces* 18(1): 3122-3139.

Gamba, O.A., Badawi, M., Said, H., Barres, O., Lainé, J., Mesquita, J. & Foucaud, Y. 2025. pH-dependent behavior of quartz surfaces: Insights from XPS, DRIFT, and potentiometric titrations. *The Journal of Physical Chemistry B* 129(37): 9517-9528.

Hoang, T.B., Stokke, B.T., Hanke, U., Johannessen, A. & Johannessen, E.A. 2019. The characterisation and quantification of immobilised concanavalin A on quartz surfaces based on the competitive binding to glucose and fluorescent labelled dextran. *Sensors* 19(2): 318.

Hucknall, A., Kim, D.H., Rangarajan, S., Toomey, R.H.L., Reichert, W.M. & Chilkoti, A. 2009. Simple fabrication of antibody microarrays on nonfouling polymer brushes with femtomolar sensitivity for protein analytes in serum and blood. *Advanced Materials* 21(19): 1968-1971.

Izunobi, J.U. & Higginbotham, C.L. 2011. Polymer molecular weight analysis by ^{1}H NMR spectroscopy. *Journal of Chemical Education* 88(8): 1098-1104.

Linssen, M.D.M.E., Liu, Y.T., van de Wijdeven, S.A.H., Tholen, M.M.E., de Jong, A.M. & Prins, M.W.J. 2024. Oriented antibody coupling to an antifouling polymer using glycan remodeling for biosensing by particle motion. *Bioconjugate Chemistry* 35(7): 996-1006.

Liu, R., De Leonardis, P., Cellesi, F., Tirelli, N. & Saunders, B.R. 2008. Cationic temperature-responsive poly(N-isopropyl acrylamide) graft copolymers: From triggered association to gelation. *Langmuir* 24(14): 7099-7106.

Lorandi, F., Fantin, M., Wang, Y., Isse, A.A., Gennaro, A. & Matyjaszewski, K. 2020. Atom transfer radical polymerization of acrylic and methacrylic acids: Preparation of acidic polymers with various architectures. *ACS Macro Letters* 9(5): 693-699.

Marcelino, T., Docampo, M.A.R., Qian, X., Ade, C., Brodszkij, E., Ceccato, M., Foss, M., Dulchavsky, M., Bardwell, J.C.A. & Städler, B. 2023. Surfaces coated with polymer brushes work as carriers for histidine ammonia lyase. *Macromolecular Bioscience* 23(8): 2200528.

Mayerhöfer, T.G. 2004. Modelling IR-spectra of single-phase polycrystalline materials with random orientation—a unified approach. *Vibrational Spectroscopy* 35(1-2): 67-76.

Muranaka, M. & Okada, T. 2009. Preparation of monodisperse polylactide microspheres by dispersion polymerization using a polymeric stabilizer with hydroxy groups. *Macromolecular Rapid Communications* 30(3): 152-156.

Ni, H., Yang, Y., Chen, Y., Liu, J., Zhang, L. & Wang, M. 2017. Preparation of a poly(DMAEMA-co-HEMA) self-supporting microfiltration membrane with high anionic permselectivity by electrospinning. *e-Polymers* 17(2): 149-157.

Popova, T.O., Zvereva, E.B. & Borisov, O.V. 2023. Interaction of polyanionic and polycationic brushes with globular proteins and protein-like nanocolloids. *Biomimetics* 8(8): 597.

Prabhakar, T., Giaretta, J., Zulli, R., Rath, R.J., Farajikhah, S., Talebian, S. & Dehghani, F. 2025. Covalent immobilization: A review from an enzyme perspective. *Chemical Engineering Journal* 503: 158054.

Sakata, S., Inoue, Y. & Ishihara, K. 2016. Precise control of surface electrostatic forces on polymer brush layers with opposite charges for resistance to protein adsorption. *Biomaterials* 105: 102-108.

Shahidan, N.N., Liu, R., Cellesi, F., Alexander, C., Shakesheff, K.M. & Saunders, B.R. 2011. Thermally triggered assembly of cationic graft copolymers containing 2-(2-methoxyethoxy)ethyl methacrylate side chains. *Langmuir* 27(22): 13868-13878.

Shin, Y.W., Roberts, J.E. & Santore, M. 2001. The influence of charge variation on the adsorbed configuration of a model cationic oligomer onto colloidal silica. *Journal of Colloid and Interface Science* 244(1): 190-199.

Soares, G.O.N., Santos, A.C., Domingos, R., Kurchaidt, R. & Gonçalves, D. 2026. Supramolecular PDDA/PEDOT:PSS biosensor for early pancreatic cancer detection via CA19-9: Clinical validation on human blood samples. *ACS Omega* 11(4): 6452-6463.

Szewczyk-Łagodzińska, M., Plichta, A., Dębowski, M., Kraszewska, S., Ibrahim, A. & Florjańczyk, Z. 2023. Recent advances in the application of ATRP in the synthesis of drug delivery systems. *Polymers* 15(5): 1234.

Tardy, B.L., Mattos, B.D., Otoni, C.G., Beaumont, M., Majoinen, J., Kämäräinen, T. & Rojas, O.J. 2021. Deconstruction and reassembly of renewable polymers and biocolloids into next generation structured materials. *Chemical Reviews* 121(22): 13661-13788.

Vetri, V., Carrotta, R., Picone, P., Di Carlo, M. & Militello, V. 2010. Concanavalin A aggregation and toxicity on cell cultures. *Biochimica et Biophysica Acta (BBA) - Proteins and Proteomics* 1804(1): 173-183.

Wang, T., Xu, T., Yang, H. & Xu, L. 2025. Protein-resistant surface coatings formed by mixed polymer brushes of fluorosiloxane and zwitterion. *Progress in Organic Coatings* 209: 109560.

Wu, H., Zhu, Y., Liu, H., Deng, Y., Wang, Z., Liu, H., Li, Z. & Ming, L. 2026. pH-responsive dual-network PVA films integrating CNC-stabilized *Mosla chinensis* essential oil emulsions for active food packaging. *Foods* 15(13): 2401.

Xu, X., Yuan, Y., Hu, G., Wang, X., Qi, P., Wang, Z., Wang, Q., Wang, X., Fu, Y., Li, Y. & Yang, H. 2017. Exploiting pH-regulated dimer-tetramer transformation of concanavalin A to develop colorimetric biosensing of bacteria. *Scientific Reports* 7(1): 1452.

Yang, H., Liu, Z., Wang, B., Xu, J., Tao, S.C. & Zhang, S. 2024. Deciphering disease through glycan codes: Leveraging lectin microarrays for clinical insights. *Acta Biochimica et Biophysica Sinica* 56(8): 1145-1155.

Yang, N. & Chang, Y. 2025. Concanavalin A-loaded chitosan nanoparticles synthesis and characterization to inhibit the proliferation of lung cancer. *Pharmacognosy Magazine* 21(2): 626-638.